

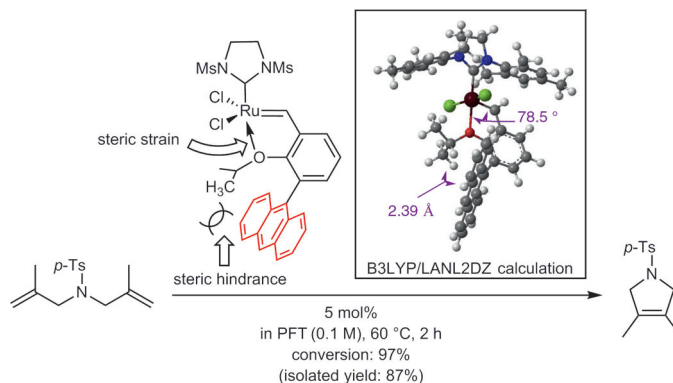
Highly Activated Second-Generation Grubbs–Hoveyda Catalyst Driven by Intramolecular Steric Strain

Yuki Kobayashi^a
 Hiroki Miyazaki^a
 Sae Inukai^a
 Chika Takagi^a
 Reo Makino^a
 Kento Shimowaki^a
 Rina Igarashi^a
 Yuya Sugiyama^a
 Shuichi Nakamura^b
 Masato Matsugi^{*a}

^a Faculty of Agriculture, Meijo University, 1-501 Shiogamaguchi, Tempaku-ku, Nagoya 468-8502, Japan
 matsugi@meijo-u.ac.jp

^b Graduate School of Engineering, Nagoya Institute of Technology, Gokiso, Showa-ku, Nagoya 466-8555, Japan

We would like to dedicate this letter to Prof. Takayuki Shioiri on his 80th birthday.



Received: 21.04.2016
 Accepted after revision: 08.06.2016
 Published online: 13.07.2016
 DOI: 10.1055/s-0035-1562468; Art ID: st-2016-u0283-l

Abstract Various Grubbs–Hoveyda second-generation catalysts activated by intramolecular steric strain were prepared. The variant bearing a 9-anthracenyl group in the ligand moiety exhibited the highest catalytic activity. The new anthracenyl-type-activated catalyst was used in a ring-closing metathesis reaction to effectively provide a 4-substituted product effectively.

Key words catalyst, metathesis, activation, ligand, steric strain

The second-generation Grubbs–Hoveyda (GH) catalyst¹ (**1a**) is one of the most frequently used catalysts in metathesis reactions in synthetic organic chemistry (Figure 1).² To date, many modifications of **1a** have been conducted to improve its catalytic activity, and some pioneering catalysts have been reported.³ Optimization of the N-heterocyclic carbene (NHC) ligand⁴ and the aromatic bidentate ligand (2-isopropoxy styrene)⁵ as well as the immobilization of **1a** onto polymers⁶ have been investigated, and a variety of attractive catalysts have been discovered.

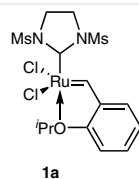


Figure 1 Second-generation Grubbs–Hoveyda catalyst

Herein, we report a novel activation method for the second-generation GH catalyst by the immobilization of the molecular conformation via the intramolecular steric strain in the ligand moiety. We then applied the catalyst with the highest activity to the catalysis of the ring-closing metathesis (RCM) reactions of tetrasubstituted olefins, which are usually difficult to achieve using second-generation GH catalysts.

We hypothesized that if an extensively spread aromatic structure was introduced in the 3-position of the 2-isopropoxy styrene ligand, an intramolecular steric hindrance would exist between the aromatic ring of the ligand moiety and the methyl of the alkoxy group (Figure 2). This steric hindrance would influence the coordination environment between the lone electron pair on the isopropoxy oxygen and ruthenium and therefore the activity of the catalyst. Actually, it has been known that the catalyst **1b** shows higher activity than GH second-generation catalyst **1a**.⁷

The catalysts prepared for this study are shown in Figure 2, and the synthetic routes for these catalysts are shown in Scheme 1. All new catalysts (**1c–f**)⁸ and the known cata-

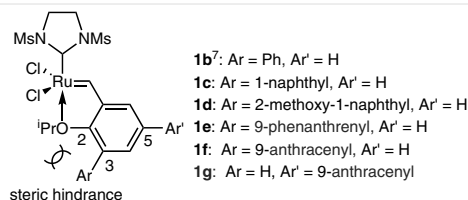
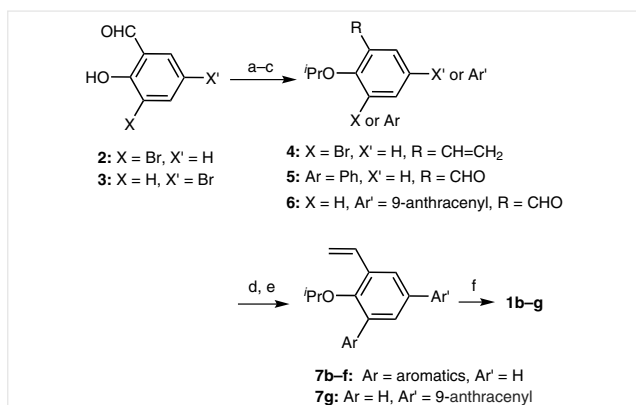


Figure 2 Second-generation Grubbs–Hoveyda catalysts expected to offer conformation control via intramolecular steric hindrance

Table 1 Chemical Shifts of the Methyl Group on the Isopropyl Function in CDCl₃ at 23 °C

Catalyst	δ (ppm)	Catalyst	δ (ppm)
1a	1.27	1d	0.79
1b	0.81	1e	0.57
1c	0.75	1f	0.77

lyst **1b**⁷ were prepared from 3-bromo-2-hydroxybenzaldehyde (**2**) in moderate yields via alkylation, Wittig reaction, Suzuki–Miyaura coupling, and successive ligand exchange with second-generation Grubbs catalyst in the presence of CuCl(I).⁹ The 5-position-substituted catalyst **1g** was also prepared from 5-bromo-2-hydroxybenzaldehyde **3** via a similar route.¹⁰



Scheme 1 Synthesis of second-generation Grubbs–Hoveyda catalysts **1b–f** bearing a biaryl ligand structure. *Reagents and conditions:* a) *i*-PrI (5.0 equiv), K₂CO₃ (8.0 equiv), DMF, 60 °C, 2 h; 99%; b) [Ph₃PMe]Br (2.3 equiv), NaHMDS (4.3 equiv), dry THF, –78 °C to 0 °C, 3 h; **4** quant.; c) ArB(OH)₂ (1.1 equiv), K₃PO₄ (5.1 equiv), *S*-Phos (0.125 equiv), Pd(OAc)₂ (0.05 equiv), THF–H₂O (2:1 v/v); reflux, 20 h; **5**, 97%; **6**, 45%; d) ArB(OH)₂ (1.1 equiv), K₃PO₄ (5.0 equiv), *S*-Phos (0.125 equiv), Pd(OAc)₂ (0.05 equiv), THF–H₂O (2:1 v/v); reflux, 3–22 h; **7c**, quant.; **7d**, 67%; **7e**, 60%; **7f**, quant.; e) NaOt-Bu (3.0–7.5 equiv), [Ph₃PMe]Br (3.0–7.5 equiv), dry Et₂O, r.t., 1 h; **7b**, 55%; **7g**, 27%; f) Grubbs II catalyst (1.0 equiv), CuCl(I) (2.0 equiv), dry CH₂Cl₂, 30 °C, 3 h; **1b**, 10%; **1c**, 35%; **1d**, 35%; **1e**, 40%; **1f**, 49%; **1g**, 67%.

As shown in Table 1, the ¹H NMR spectra of **1b–f** indicated that the chemical shifts of the methyl group on the isopropoxy moiety are quite different from that of the original second-generation GH catalyst **1a** (δ = 0.57–0.81 ppm vs. δ = 1.27 ppm). This finding suggests that all the isopropoxy groups of **1b–f** experience quite different environments due to the shielding effect. The catalysts bearing bicyclic or tricyclic aromatic function showed higher field shifts than monocyclic **1b**, and a strong shielding effect was observed in the catalyst **1e**, the ligand that has an angularly distributed π-conjugated system.

RCM reactions using diethyl 2-allyl-2-(2-methylallyl)malonate¹¹ (**8**) were examined to confirm the relative catalytic activities of the prepared catalysts. The reactions were conducted with CDCl₃ as the solvent to allow NMR monitoring of the reaction aliquots. At certain reaction times, the conversion (%) of the reaction was determined by recording ¹H NMR spectra of reaction mixtures and calculating the relative integrals of the corresponding olefinic protons of product **9**. Interestingly, a strong difference in catalytic activity was observed between **1a** and catalysts **1b–f** (Figure 3). The result clearly indicates that the introduction of a polycyclic aromatic moiety at the 3-position on the aromatic ligand is an effective means of achieving significant activation of second-generation GH catalysts. Importantly, we found that the introduction of a 9-anthracenyl functional group led to a strong acceleration of RCM catalysis. Indeed, **1f** showed the highest activity among the catalysts examined. The catalytic activity was extremely low when the 5-position-substituted catalyst **1g** was used.

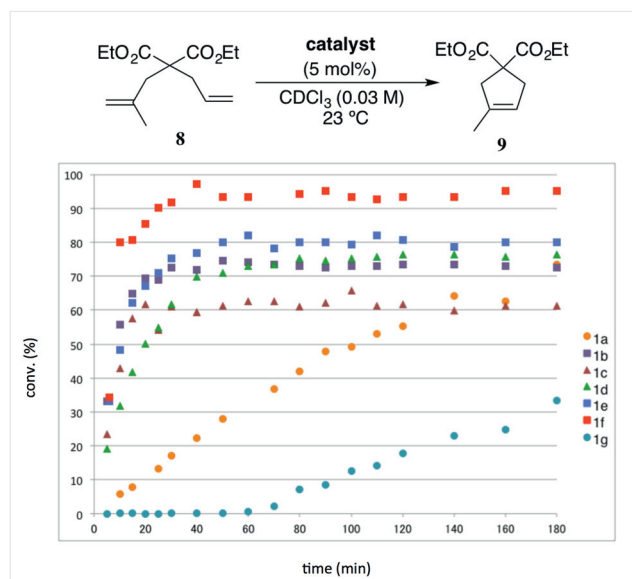
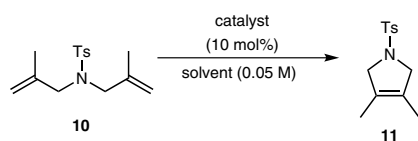


Figure 3 RCM reactions of diethyl 2-allyl-2-(2-methylallyl)malonate **8** in CDCl₃ at 23 °C

These findings led us to hypothesize that catalyst **1f** could effectively catalyze RCM reactions of tetrasubstituted olefins, which are usually difficult to achieve using second-generation GH catalysts. We compared the catalytic activities of second-generation GH catalyst **1a** and catalyst **1f** in an RCM reaction using 4-methyl-*N,N*-bis(2-methylallyl)benzenesulfonamide^{4a} **10** as a substrate (Table 2).¹² As expected, catalyst **1f** showed a higher catalytic activity than the original catalyst **1a**. The reaction employing **1f** afforded the tetrasubstituted RCM product **11** in 75% yield after 24 hours, whereas **1a** afforded the product in 5% yield under same reaction conditions (Table 2, entries 1, 2). Importantly, these results show that a dramatic improvement in acti-

vation can be achieved by simply introducing an anthracenyl functional group to the ligand. Interestingly, accelerated reactivity and increased yield were achieved when the RCM reaction of **10** was conducted in a fluororous solvent (Table 2, entries 4 and 5).¹² Among the solvents studied, perfluorotoluene (PFT) exhibited the highest reactivity (Table 2, entry 7).¹³ Although benzotrifluoride (BTF) was a more effective solvent than toluene, the activation achieved was inferior that achieved using PFT. We found that 5 mol% of the catalyst was sufficient to complete the RCM reaction when 0.1 M of the reactant was used in PFT. A satisfactory conversion of 97% was obtained in this case (Table 2, entry 10).

Table 2 Ring-Closing Metathesis Reactions of 4-Methyl-*N,N*-bis(2-methylallyl) Benzenesulfonamide **11**



Entry	Catalyst	Solvent	Temp (°C)	Time (h)	Conv (%) ^a
1	1a	CH ₂ Cl ₂	reflux	24	5
2	1f	CH ₂ Cl ₂	reflux	24	75
3	1f	toluene	60	10	69
4	1f	BTF	60	10	89
5	1f	PFT	60	10	100
6	1f	BTF	60	1	73
7	1f	PFT	60	1	88
8 ^b	1f	PFT	60	2	56
9 ^b	1f	PFT	60	24	53
10 ^{b,c}	1f	PFT	60	2	97 (87) ^d

^a Determined by ¹H NMR spectroscopy.

^b The concentration of **1f** was 5 mol%.

^c Reactant concentration was 0.1 M.

^d Isolated yield.

Molecular orbital calculations (B3LYP/LANL2DZ)¹⁴ of catalyst **1f** were conducted for conformational analysis. As shown in Figure 4, the CH moiety of the methyl group was found to be located close to the π -face of the anthracenyl group. The closest interatomic distance between the CH moiety and the aromatic π -plane was shorter (2.39 Å) than the sum of the individual van der Waals radii.¹⁵ Consistent with the MO calculation, the NOESY spectrum of the catalyst **1f** in CDCl₃ indicate a small distance between the CH moiety of the methyl group and the π moiety (see Supporting Information). The calculated bond angle¹⁴ (O–Ru–C) was 78.5°. It was a fairly narrow angle compared with the corresponding angle of the X-ray data¹⁶ of the original second-generation GH catalyst **1a**.¹⁷

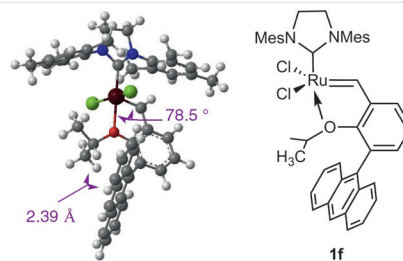
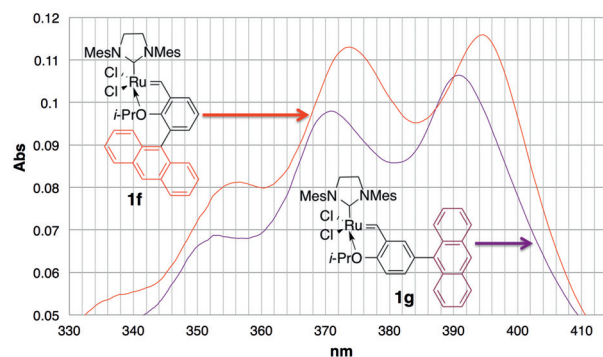


Figure 4 Conformation of **1f** based on B3LYP/LANL2DZ calculations as implemented in Gaussian 03

We speculate the possibility of the presence of an intramolecular CH– π interaction¹⁸ between isopropyl group and aromatic moiety. It is an intermolecular interaction between a CH moiety and a π plane, which was proposed by Nishio et al. in 1977.¹⁹ The calculation data of the shorter distance than the sum of the individual van der Waals radii strongly supports the existence of this interaction.

Most importantly, as shown in Table 3, the maximum UV-Vis absorption wavelengths of catalyst **1f** were red-shifted relative to those of the 5-position-substituted isomer **1g** ($\lambda_{\text{max}} = 394.6, 373.8, 356.4$ nm and $\lambda_{\text{max}} = 390.8, 370.8, 353.2$ nm, respectively).^{18c} Meanwhile, the maximum UV-Vis absorption wavelengths of the bidentate ligand precursors of **1f** and **1g** were almost the same (see Supporting Information). These UV-Vis data support an orbital interaction, and the red shift is evidence of a CH– π interaction in **1f**.²⁰ Although more definitive evidence of the interaction could be obtained by X-ray crystallographic analysis of the catalyst **1f**, we were unable to obtain suitable single crystals.

Table 3 UV-Vis Spectrum of **1f** and the Regioisomer **1g** in Chloroform^a



Catalyst	λ_{max} (nm)		
1f	394.6	373.8	356.4
1g	390.8	370.8	353.2

^a The solution concentration was $1.25 \cdot 10^{-2}$ M.

An activation mechanism considering the rate-determining step of RCM reactions using second-generation GH catalysts has been reported by the Grubbs and Gladysz groups.²¹ According to their report, the rate-determining step is the release of the bidentate ligand on ruthenium, and the reaction rate is thus influenced by the ligation ability of the original ligand in the molecule.²² Similarly, we attribute the effective activation of the catalysts in part to the decrease in the ligation ability on ruthenium. These bidentate ligands **7b–f** would experience steric strain due to the intramolecular CH– π interaction, which requires a highly ordered conformation, and would thus release the ligand more easily than the original second-generation GH catalyst.

In summary, we have prepared modified second-generation GH catalysts activated by the remarkable intramolecular steric strain. The catalyst **1f** exhibited the highest catalytic activity, and we have shown that catalyst **1f** can be used successfully in an RCM reaction to generate a 4-substituted product. We believe that catalyst **1f** is one of the most useful second-generation GH type catalysts because of its ease of derivation from the original catalyst and superior catalytic activity.

Acknowledgment

This work was supported by JSPS KAKENHI Grant Number 26450145, and Prof. Uozumi's JST-ACCEL program.

Supporting Information

Supporting information for this article is available online at <http://dx.doi.org/10.1055/s-0035-1562468>.

References and Notes

- (1) Kingsbury, J. S.; Harrity, J. P. A.; Bonitatebus, P. J.; Hoveyda, A. H. *J. Am. Chem. Soc.* **1999**, *121*, 791.
- (2) (a) Fürstner, A. *Alkene Metathesis in Organic Synthesis*; Springer: New York, **1998**. (b) Grubbs, R. H. *Handbook of Metathesis*; Wiley-VCH: Weinheim, **2003**. (c) Wang, H.; Matsubashi, H.; Doan, B. D.; Goodman, S. N.; Ouyang, X.; Clark, W. M. *Tetrahedron* **2009**, *65*, 6291. (d) Kong, J.; Chen, C.; Padros, J. B.; Cao, Y.; Dunn, R. F.; Dolman, S. J.; Janey, J.; Li, H.; Zacuto, M. *J. Org. Chem.* **2012**, *77*, 3820.
- (3) For selected reviews, see: (a) Fürstner, A. *Angew. Chem. Int. Ed.* **2000**, *39*, 3012. (b) Connon, S. J.; Blechert, S. *Angew. Chem. Int. Ed.* **2003**, *42*, 1900. (c) Clavier, H.; Grela, K.; Kirschning, A.; Mauduit, M.; Nolan, S. P. *Angew. Chem. Int. Ed.* **2007**, *46*, 6786. (d) Samojłowicz, C.; Bieniek, C.; Grela, K. *Chem. Rev.* **2009**, *109*, 3708. (e) Higman, C. S.; Lummiss, J. A. M.; Fogg, D. E. *Angew. Chem. Int. Ed.* **2016**, *55*, 3552.
- (4) For selected examples, see: (a) Berlin, J. M.; Campbell, K.; Ritter, T.; Funk, T. W.; Chlenov, A.; Grubbs, R. H. *Org. Lett.* **2007**, *9*, 1339. (b) Kuhn, K. M.; Bourg, J.-B.; Chung, C. K.; Virgil, S. C.; Grubbs, R. H. *J. Am. Chem. Soc.* **2009**, *131*, 5313. (c) Petit, L. V.; Clavier, H.; Linden, A.; Blumentritt, S.; Nolan, S. P.; Dorta, R. *Organometallics* **2010**, *29*, 775. (d) Leitgeb, A.; Abbas, M.; Fischer, R. C.; Poater, A.; Cavallo, L.; Slugovc, C. *Catal. Sci. Technol.* **2012**, *2*, 1640. (e) Sauer, D. F.; Himiyama, T.; Tachikawa, K.; Fukumoto, K.; Onoda, A.; Mizohata, E.; Inoue, T.; Boccola, M.; Schwaneberg, U.; Hayashi, T.; Okuda, J. *ACS Catal.* **2015**, *5*, 7519.
- (5) For selected examples, see: (a) Zaja, M.; Connon, S. J.; Dunne, A. M.; Rivard, M.; Buschmann, N.; Jiricek, J.; Blechert, S. *Tetrahedron* **2003**, *59*, 6545. (b) Dragutan, V.; Dragutan, I. *Platinum Met. Rev.* **2005**, *49*, 33. (c) Barbasiewicz, M.; Bieniek, M.; Michrowska, A.; Szadkowska, A.; Makal, A.; Woźniak, K.; Grela, K. *Adv. Synth. Catal.* **2007**, *349*, 193. (d) Matsugi, M.; Kobayashi, Y.; Suzumura, N.; Tsuchiya, Y.; Shioiri, T. *J. Org. Chem.* **2010**, *75*, 7905. (e) Olszewski, T. K.; Bieniek, M.; Skowerski, K.; Grela, K. *Synlett* **2013**, *24*, 903.
- (6) For selected examples, see: (a) Allen, D. P.; Wingerden, M. M. V.; Grubbs, R. H. *Org. Lett.* **2009**, *11*, 1261. (b) Cheong, J. L.; Wong, D.; Lee, S.-G.; Lim, J.; Lee, S. S. *Chem. Commun.* **2015**, *51*, 1042. (c) Chen, S.-W.; Zhang, Z.-C.; Zhai, N.-N.; Zhong, C.-M.; Lee, S.-G. *Tetrahedron* **2015**, *71*, 648. (d) Skowerski, K.; Białocki, J.; Czarnocki, S. J.; Żukowska, K.; Grela, K. *Beilstein J. Org. Chem.* **2016**, *12*, 5.
- (7) Wakamatsu, H.; Blechert, S. *Angew. Chem. Int. Ed.* **2002**, *41*, 2403.
- (8) **Characterization Data of Catalyst 1c**
Green crystal, mp 169.0–171.5 °C. ¹H NMR (270 MHz, CDCl₃): δ = 0.75 (dd, J = 52.1, 6.2 Hz, 6 H), 2.50 (br s, 18 H), 4.06–4.18 (m, 5 H), 5.30 (s, 1 H), 6.96–7.06 (m, 6 H), 7.34–7.44 (m, 5 H), 7.76–7.82 (m, 3 H), 16.72 (s, 1 H). ¹³C NMR (68 MHz, CDCl₃): δ = 18.5, 20.6, 21.0, 51.4, 77.7, 122.7, 123.1, 125.1, 126.1, 126.4, 127.0, 127.4, 128.0, 128.3, 128.4, 129.3, 131.9, 133.0, 138.8, 147.7, 149.8, 211.3, 299.3. IR: 2918, 1558, 1476, 1420, 1255, 1193, 1032, 777, 733, 646 cm⁻¹. HRMS (FAB⁺): m/z calcd for C₄₁H₄₅Cl₂N₂ORu: 754.1952; found: 754.1942.
Characterization Data of Catalyst 1d
Green crystal, mp 172.5–173.2 °C. ¹H NMR (270 MHz, CDCl₃): δ = 0.67 (d, J = 6.21 Hz, 3 H), 0.90–0.93 (m, 3 H), 2.50 (br s, 18 H), 3.79 (s, 3 H), 4.15 (s, 4 H), 4.20–4.24 (m, 1 H), 6.93–7.04 (m, 4 H), 7.24–7.35 (m, 5 H), 7.48–7.54 (m, 2 H), 7.69–7.75 (m, 1 H), 7.82 (d, J = 9.18 Hz, 1 H), 16.64 (s, 1 H). ¹³C NMR (68 MHz, CDCl₃): δ = 18.5, 20.8, 21.1, 51.6, 56.1, 77.8, 112.6, 121.8, 122.7, 122.9, 133.5, 135.7, 138.7, 147.5, 150.6, 153.7, 211.9, 299.5. HRMS (FAB⁺): m/z calcd for C₄₂H₄₇Cl₂N₂O₂Ru: 784.2058; found: 784.2106.
Characterization Data of Catalyst 1e
Green crystal, mp 163.7–165.0 °C. ¹H NMR (270 MHz, CDCl₃): δ = 0.77 (dd, J = 62.6, 5.9 Hz, 6 H), 2.52 (br s, 18 H), 4.17–4.28 (m, 5 H), 6.95–7.03 (m, 6 H), 7.39–7.42 (m, 1 H), 7.50–8.71 (m, 8 H), 8.67 (d, J = 8.1 Hz, 2 H), 16.94 (s, 1 H). ¹³C NMR (68 MHz, CDCl₃): δ = 20.4, 21.1, 21.3, 52.4, 77.8, 122.5, 123.0, 123.3, 126.8, 126.9, 127.0, 127.5, 127.7, 128.8, 130.3, 131.1, 131.3, 134.7, 136.3, 138.8, 147.5, 149.9, 211.3, 298.9. IR: 2920, 1480, 1424, 1255, 1203, 1097, 921, 851, 745, 720 cm⁻¹. HRMS (FAB⁺): m/z calcd for C₄₅H₄₇Cl₂N₂ORu: 804.2187; found: 804.2195.
Characterization Data of Catalyst 1f
Green crystal, mp 172.3–173.7 °C. ¹H NMR (270 MHz, CDCl₃): δ = 0.57 (d, J = 6.2 Hz, 6 H), 2.52 (br s, 18 H), 3.82–3.92 (m, 1 H), 4.17 (s, 4 H), 6.96–7.10 (m, 6 H), 7.33–7.81 (m, 6 H), 7.88 (d, J = 36.5 Hz, 2 H), 7.98 (d, J = 1.6 Hz, 2 H), 8.43 (s, 1 H), 16.77 (s, 1 H). ¹³C NMR (68 MHz, CDCl₃): δ = 18.4, 21.1, 21.4, 51.4, 78.6, 123.0, 123.0, 125.3, 125.4, 126.4, 127.0, 127.5, 128.2, 129.4, 130.2, 131.0, 133.0, 135.9, 147.8, 150.8, 211.3, 298.7. IR: 2917, 1481,

- 1443, 1255, 1197, 1098, 1014, 925, 886, 851, 732 cm^{-1} . HRMS (FAB⁺): m/z calcd for $\text{C}_{45}\text{H}_{47}\text{Cl}_2\text{N}_2\text{ORu}$: 804.2187; found: 804.2167.
- (9) Garber, S. B.; Kingsbury, J. S.; Gray, B. L.; Hoveyda, A. H. *J. Am. Chem. Soc.* **2000**, *122*, 8168.
- (10) **Characterization Data of Catalyst 1g**
Green crystal, mp 300 °C (dec.). ¹H NMR (270 MHz, CDCl_3): δ = 1.33 (d, J = 5.7 Hz, 6 H), 2.11–2.42 (br m, 18 H), 4.10 (s, 4 H), 4.92–5.01 (m, 1 H), 6.93–6.97 (m, 6 H), 7.28–7.50 (m, 6 H), 7.68 (d, J = 8.9 Hz, 2 H), 7.98 (d, J = 8.4 Hz, 2 H), 8.43 (s, 1 H), 16.64 (s, 1 H). ¹³C NMR (68 MHz, CDCl_3): δ = 21.1, 21.4, 112.9, 125.1, 125.3, 125.5, 126.7, 127.3, 128.3, 129.5, 130.7, 131.4, 132.4, 132.6, 135.6, 139.0, 145.4, 152.0, 211.0, 296.4. HRMS (FAB⁺): m/z calcd for $\text{C}_{45}\text{H}_{48}\text{Cl}_2\text{N}_2\text{ORu}$: 804.2162; found: 804.2187.
- (11) Kobayashi, Y.; Inukai, S.; Kondo, N.; Watanabe, T.; Sugiyama, Y.; Hamamoto, H.; Shioiri, T.; Matsugi, M. *Tetrahedron Lett.* **2015**, *56*, 1363.
- (12) Fustero, S.; Fuentes, A. S.; Barrio, P.; Haufe, G. *Chem. Rev.* **2015**, *115*, 871.
- (13) Samojłowicz, C.; Bieniek, M.; Pazio, A.; Makal, A.; Woźniak, K.; Poater, A.; Cavallo, L.; Wójcik, J.; Zdanowski, K.; Grela, K. *Chem. Eur. J.* **2011**, *17*, 12981.
- (14) For B3LYP, see: (a) Becke, A. D. *J. Chem. Phys.* **1993**, *98*, 5648. For LANL2DZ, see: (b) Dunning, T. H.; Hay, P. J. *Modern Theoretical Chemistry*; Vol. 3; Plenum Press: New York, **1977**. (c) Hay, P. J.; Wadt, W. R. *J. Chem. Phys.* **1985**, *82*, 270. (d) Hay, P. J.; Wadt, W. R. *J. Chem. Phys.* **1985**, *82*, 299.
- (15) Bondi, A. *J. Phys. Chem.* **1964**, *68*, 441.
- (16) Garber, S. B.; Kingsbury, J. S.; Gray, B. L.; Hoveyda, A. H. *J. Am. Chem. Soc.* **2000**, *122*, 8168.
- (17) The bond angle (O–Ru–C) of **1a** was 79.0° (79.3° in X-ray) when calculated in the same method.
- (18) For selected reviews, see: (a) Oki, M. *Acc. Chem. Res.* **1990**, *23*, 351. (b) Nishio, M.; Umezawa, Y.; Hirota, M.; Takeuchi, Y. *Tetrahedron* **1995**, *51*, 8665. (c) Nishio, M.; Umezawa, Y.; Hirota, M. *The CH/π Interaction*; Wiley-VCH: Weinheim, **1998**.
- (19) Nishihata, K.; Nishio, M. *Tetrahedron Lett.* **1977**, *18*, 1041.
- (20) Matsugi, M.; Itoh, K.; Nojima, M.; Hagimoto, Y.; Kita, Y. *Chem. Eur. J.* **2002**, *8*, 5551.
- (21) (a) Sanford, M. S.; Ulman, M.; Grubbs, R. H. *J. Am. Chem. Soc.* **2001**, *123*, 749. (b) da Costa, R. C.; Gladysz, J. A. *Chem. Commun.* **2006**, 2619.
- (22) (a) Love, J. A.; Sanford, M. S.; Day, M. W.; Grubbs, R. H. *J. Am. Chem. Soc.* **2003**, *125*, 10103. (b) Trzaskowski, B.; Grela, K. *Organometallics* **2013**, *32*, 3625.